B10

Proceedings of the 5th International Conference on Inverse Problems in Engineering: Theory and Practice, Cambridge, UK, 11-15th July 2005

ANALYSIS OF THE FIELD SYNTHESIS ALGORITHM, VARIABLE FIELD GENERATION, USING MAGNETOSTATIC FINITE ELEMENT METHOD AND OPTIMIZATION

N. BROOKS [1], F. GROSS [2] and T. BALDWIN [1]
[1] *Center for Advanced Power Systems, Florida A&M University, Tallahassee, Florida, 32307, USA*
email: nbrooks@magnet.fsu.edu, baldwin@caps.fsu.edu
[2] *Department of Electrical & Computer Engineering, FAMU-FSU College of Engineering, Tallahassee, Florida, 32307, USA*
email: gross@eng.fsu.edu

Abstract – An overview of the magnetostatic field synthesis method, Variable Field Generation (VFG), and results from applying it to a test case to design magneto-plasma-aerodynamic (MPAD) devices to observe algorithm performance in the MATLAB programming environment are presented in this paper. The algorithm applied to this test case included integrating the Magnetostatic module of the finite element software package, Maxwell 3D by Ansoft, for design verification and optimization.

1. INTRODUCTION

Analysis of various hypersonic system concepts for future advanced air vehicles indicates that the benefits of magnetic field systems are significant. This vehicle will produce an ionized or plasma environment around the aircraft using on-board e-beam generators (combination of laser and microwave energy). In addition magnetic devices will be on-board to provide the needed magnetic field to induce the desired Lorentz force. The effect of this force can manipulate the plasma around a given surface to improve flight efficiency, maneuverability, and enable advanced flight control. An essential task in the design of this aircraft's MPAD system is that once the appropriate field patterns have been determined, the derivation of the proper magnetic configurations needed on the aircraft must be undergone. Therefore, there exists a need to provide a magnetic design solution or set of solutions for a MPAD system that will aid in hypersonic and trans-atmospheric travel of future air vehicles. The need for uniform field patterns over large surfaces and/or the ability to quickly alter the field pattern requires unique and inventive magnetic designs that may not have been ever created. Trial and error experimentation using various electromagnet or permanent magnet designs would be extremely inefficient and, therefore, alternative design methods must be used. Finding solutions of design problems like that can be attempted using different mathematical and engineering techniques. Many of these techniques are limited to specific problems and rely on some form of simplification or symmetry in solving familiar problems in engineering or physics. The distinctiveness of this research is an implementation of these techniques in a general design methodology to solve for arbitrary field configurations, instead of relying strictly on intuition or common design practices to iteratively conceive, evaluate, and correct designs. This approach is to reverse engineer the design, based on the desired fields to be produced. An inverse scheme that is versatile and autonomous in its application to synthesize MPAD systems derived from magnetic field requirements would aid the designer in producing an optimal design.

Therefore, in order to provide the ability to satisfy unique magnetic field pattern requirements, field synthesis methods have been employed to inversely determine the necessary magnetic source configurations. These methods require a physical model, mathematical model, a means to evaluate the state of this mathematical model, and a method to solve the system of equations produced by the previous processes. Based on these requirements, the method of VFG has been developed. This method provides field synthesis with the niche ability of creating a system that produces an alterable magnetostatic field pattern. This capability is promising for future hypersonic aerospace technologies. Ultimately, the algorithm inversely determines the type, geometry, orientation, configuration, and other physical properties of electromagnetic sources that will produce a desired magnetic field, with the specific capability to generate a design solution that is able to fulfill multiple field pattern requirements. The performance goals of this algorithm were that it is versatile enough to facilitate design solutions for a wide-range of field patterns, yet autonomous enough to promote ease of use by non-specialist in inverse methods.

This paper provides an overview of the developed algorithm, discussing the methods employed, and outlines the process of employing this algorithm to solve the inverse problem of synthesizing a magnetostatic field pattern suitable for MPAD applications.

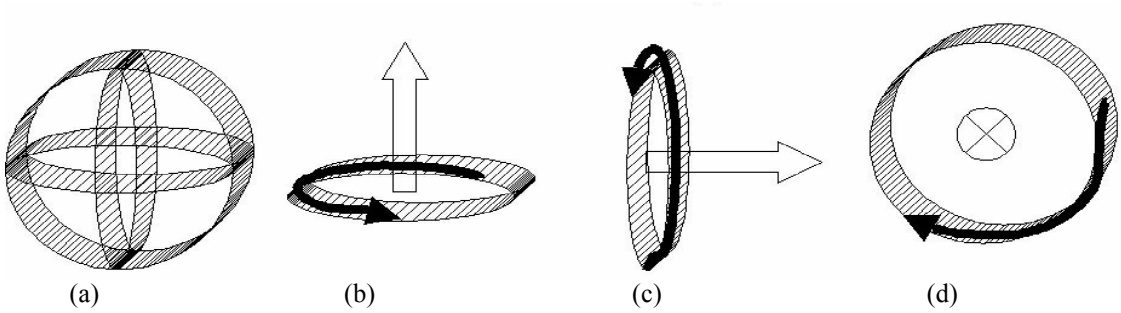

Figure 1: Illustration of VFG globe's variable field vector. (a) VFG glove serves as model for unknown magnetic source. (b) – (d) Current in each loop generates field in one of the three spatial directions.

2. VARIABLE FIELD GENERATION (VFG)

First introduced in [2], VFG is a source-modeling algorithm that defines any region of unknown magnetic sources as a system of variable sources. This source is characterized by three orthogonal current loops centered within each other, see Figure 1. This small "globe" has the ability to direct its dipole moments in any direction with the manipulation of each loops individual current. Each loop's field is in one of the Cartesian directions (either x, y, or z). Therefore, the resulting field vector of the source depends on each vector's magnitude. The result of this system is that the inverse problem of synthesizing a desired field pattern utilizes an assumed model composed only of current loops. The superposition of these current loops represents variably directed dipole fields as a basis for producing alterable field patterns for MPAD applications. Consequently, compensation magnets used on naval helicopters employ the same principle. As seen in Figure 2(a), coils are energized to cancel out magnetic noise of the aircraft. The use of such coils comes from the ability to control the production of dipole fields in all three orthogonal directions. In the naval helicopter application, the required energizing currents are determined by iterative field measurement and correction. However, the VFG method inversely computes the required energizing currents for a matrix of these coils, to produce desired field patterns. Using the physical model of a set of current loops allows for the use of a fully parameterized model for the creation of a design solution. Because this fully parameterized model consists of a variable source like that of other source searching models, the range of synthesis solutions for various magnetic field distributions is increased beyond that of traditional synthesis methods that utilize less "a priori" information. However, unlike other source-modeling methods, this variable source will not be converted to an equivalent current distribution or other conventional magnetic source. Doing so would forfeit the innate ability to generate a wide range of fields. Instead the inverse solution of the source excitations can be constructed and implemented straightforwardly into a matrix of sources as shown in Figure 2(b). The result is the ability to generate multiple field patterns from a single system, conceptually a variable magnetic field generator.

The original implementation of the concept of using orthogonal loops of current to variably orientate fields utilized an analytical expression. A closed solution of the magnetic flux density of a current carrying loop has

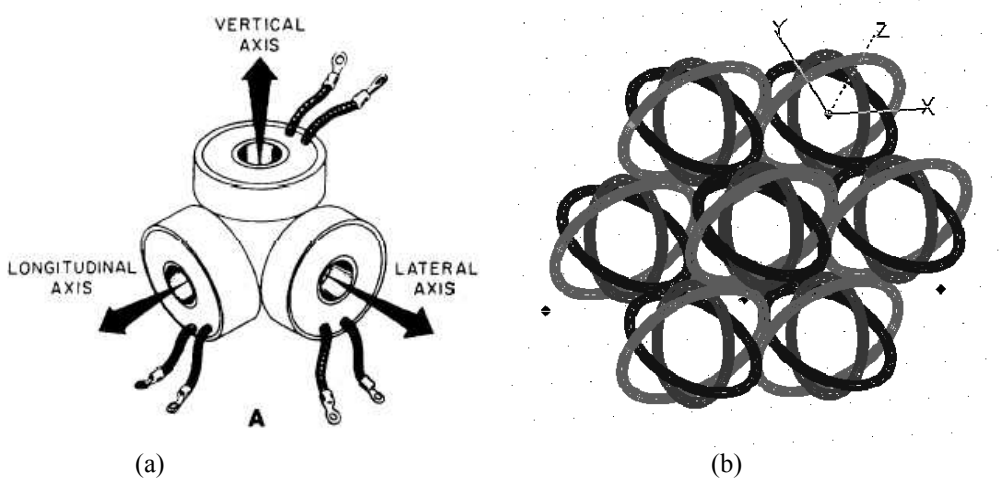

Figure 2: VFG source model (a) compensation coils for canceling magnetic noise, and (b) proposed matrix of VFG sources for field generator.

been derived, see (1) - (3), using the magnetic vector potential form of the Biot-Savart law. As described in [3], these equations provide the magnetic flux density at any point given by (x, y, z), where r is the radial distance from the axis of a circular loop, carrying current I and of radius a, namely

$$B_\eta = I\frac{\mu_0}{2\pi\sqrt{Q}}\left[E(k)\frac{1-\alpha^2-\beta^2}{Q-4a}-K(k)\right] \tag{1}$$

$$B_\psi = I\frac{\psi\ \mu_0\ \gamma}{2\pi\ a\sqrt{Q}}\left[E(k)\frac{1+\alpha^2+\beta^2}{Q-4a}-K(k)\right], \tag{2}$$

$$B_\zeta = I\frac{\zeta\ \mu_0\ \gamma}{2\pi\ a\sqrt{Q}}\left[E(k)\frac{1+\alpha^2+\beta^2}{Q-4a}-K(k)\right], \tag{3}$$

where

$$\alpha=\frac{r}{a},\quad \beta=\frac{\eta}{a},\quad \gamma=\frac{\eta}{r},\quad Q=(1+\alpha)^2+\beta^2,\quad k=\sqrt{\frac{4\alpha}{Q}},$$

and

$$\langle \eta \quad \psi \quad \zeta \rangle \in f(x,y,z).$$

$K(k)$ is the complete elliptic integral function of the 1st kind of modulus k and $E(k)$ is the complete elliptic integral function of the 2nd kind of modulus k. The permeability of free space is μ_o. The function f reassigns the Cartesian coordinates (x, y, z) to the local coordinate system (η, ψ, ς) dependent on the plane in which the loop lies. The result of this function is such that η is the Cartesian coordinate that is orthogonal to the plane of the loop. The coordinates ψ and ς are the Cartesian coordinates of the plane in which the loop lies, assigned so that the right-hand rule, $\eta = \psi \times \varsigma$, is satisfied. Figure 3 illustrates the geometry specified by (1) to (3) for a single loop. However, the algorithm models a region of unknown magnetic sources as a matrix of the m number of "globe" sources. The system of equations defining this matrix for a field measured at n points is assembled from (1) - (3). They form the vector field at the i-th measuring point (x_i, y_i, z_i) in space due to a current-carrying loop lying in any Cartesian plane as

$$\overline{B_i} \in g\left(B_\eta, B_\psi, B_\zeta\right), \tag{4}$$

where the function *g* reverses the mapping of *f*, transforming the flux densities in the local coordinate system to a 3 by 1 Cartesian vector in the reference coordinate system.

To build the governing system matrices, the field matrix of the *k*-th globe in the system must be formed using (4). The contribution of each of the three current loops designated Φ, Ω, and Θ that comprise one globe must be accounted for, as follows:

$$\mathbf{B}_{3n\times 3}^{k} = \begin{bmatrix} \overline{B}_{1}^{\Phi} & \overline{B}_{1}^{\Omega} & \overline{B}_{1}^{\Theta} \\ \vdots & \vdots & \vdots \\ \overline{B}_{n}^{\Phi} & \overline{B}_{n}^{\Omega} & \overline{B}_{n}^{\Theta} \end{bmatrix} \tag{5}$$

and each globe in the matrix becomes a column vector in the total VFG system matrix,

$$\mathbf{B}_{\mathbf{sys}}^{3n\times 3m} = \begin{bmatrix} \mathbf{B}_{3n\times 1}^{1} & \mathbf{B}_{3n\times 1}^{2} & \cdots & \mathbf{B}_{3n\times 1}^{m-1} & \mathbf{B}_{3n\times 1}^{m} \end{bmatrix}. \tag{6}$$

The summation along the columns of $\mathbf{B}_{\mathbf{sys}}$ will result in the total magnetic flux density at all measured points. Once the system matrix in (6) has been assembled, the variables must be extracted. Advantageously, the only unknown variables of (1) – (3) are the loop currents and radius. Therefore, only the radii and currents of each globe must be solved. For cases in which the radius are known parameters, extracting the current, ***I***, results in the following linear algebra equation for the fields at every measurement point:

$$\sum_{columns} \mathbf{B}_{\mathbf{sys}} = \mathbf{B}_{\mathbf{total}}^{3n\times 1} = \mathbf{C}_{3n\times 3m} \times \mathbf{I}_{3m\times 1} \,, \tag{7}$$

where **C** is the coefficient matrix representing the geometrical information of the system of VFG sources. Since the currents are the unknown variables, **C** is directly constructed using (1) – (6), except that the current ***I*** is extracted from (1) – (3). The result is the linear relationship between the total field distribution $\mathbf{B}_{\mathbf{total}}$ and the current of each loop, **I**, based on the specified radius and positioning of the source, as expressed in (7).

An alternative to the original system of equations of the infinitely thin conductor source model is that of finite radius conductors. Consequently, there is no analytical mathematical model to provide the complete field distribution of a finite radius conductor loop, only Maxwell's magnetostatic equations. Therefore, the Ansoft developed finite element analysis (FEA) software, Maxwell 3D, was utilized to evaluate the system. To remain consistent with the objectives of providing an autonomous and versatile algorithm, the complete automation of invoking the software, creating the project, defining the geometry, characterizing the model, setting the software

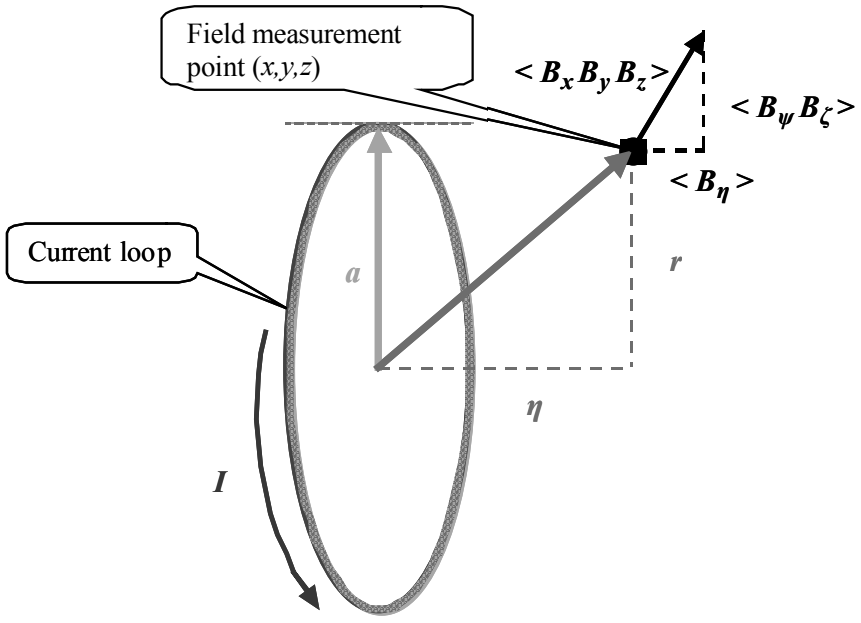

Figure 3: Geometry for source loop used in mathematical model of infinitely thin-wired physical model.

options, solving the problem, and extracting the field results was accomplished to enable the same functionality of the analytical model. The challenge here was that Maxwell 3D is not ideally constructed for such automation beyond the basic macros for repeatable processes or batch processing of pre-defined cases. Figure 4 illustrates the complex use of MATALB m-files, Maxwell 3D commands from the DOS prompt, and Maxwell 3D macros to integrate FEA into the algorithm code to evaluate the field production of the VFG matrix composed of finite radius conductor sources. The final result of this integration effort is that the design variables of the system are utilized to construct a three-dimensional CAD-like model of each of the three loops in a single source. This model is then solved using the finite element method and the resulting fields for each current loop are returned to the algorithm as the field solution, $\mathbf{B}_{\mathbf{sys}}$. $\mathbf{B}_{\mathrm{sys}}$ is then translated from the local coordinate system of each source's position within the matrix system to the global coordinate system of the problem to provide $\mathbf{B}_{\mathbf{total}}$. The result is the same relationship expressed in (7). To simplify the extraction of **I** as an unknown, the field solutions are computed at a current excitation of 1 Amp; allowing $\mathbf{B}_{\mathbf{total}}$ to be equivalent to the coefficient matrix, **C.**

The use of conductors with cross sectional area results in each loop of the source now having a different radius as opposed to the infinitely thin loop model which allowed each loop to have the same radius. Therefore the following parameter names will be used:

- *VFG matrix dimensions* is the $\mathbf{m}\times\mathbf{n}\times\mathbf{p}$ number of sources used to compose a matrix of VFG sources,
- *VFG loop order* is the ordering of which planar loop is the innermost, outermost, or middle inscribed loop of a VFG source,
- *conductor model type* determines whether the source modeled in Maxwell 3D is made from copper or a perfect conductor (to represent superconducting material),
- *VFG source radius* is the radius of the outermost loop of a VFG source, and
- *conductor radius* is the radius of the conductors used in each of the three loops of a VFG source (for the infinitely thin models this variable represents the spacing between each loop).

Whether the analytical eqns of (1) – (3) or Maxwell 3D FEA are used within the algorithm, the coeffecient matrix, **C**, containing the geometrical information of the system of sources can be computed by specifying the parameters listed above.

Applying VFG to solve any inverse magnetostatic problem requires the input of the desired flux density vectors at each point in space along with the volume of space reserved for the magnetic system. Depending on how many parameters are set as variables by the user, the algorithm solves the field synthesis problem by determining the system variables of **C** and the system excitation of **I** to provide a resultant field distribution $\mathbf{B}_{\mathbf{total}}$ equivalent to the field distribution specified. This process requires a solver to be employed to inversely solve (7). Ordinarily, an appropriate optimization routine would suffice. However, magnetic field problems inherently contain equations of the Fredholm integral type, which are ill-conditioned. The same holds true for the equations computing the field production anywhere in space of a current carrying loop, which in its simplified and closed form, (1) – (3), contains elliptic integrals. Therefore, regularization methods are usually employed to overcome the obstacles in inverting ill-conditioned systems. However, because of the many parameters that can be variables, the solution process has been refined, as the overall algorithm has been developed, to its current state. Foremost, selecting any system parameter as an unknown variable requires a nonlinear solver to find the solution of (7). Due to computational speed and resource constraints, the first decision was to define a linear problem during the process as much as possible. Therefore, the approach is to continually shrink the domain of possible design variables that will provide the best solution. The result is a process that includes three separate solution phases. Each phase identifies a set of parameters that provides the best performance using the most appropriate solver to optimize computational time. The results of a comparative study to determine the most efficient solver to apply to the system of eqns of (1) – (3) for various problems were presented in a previous paper, [4]. The use of optimization routines, such as the nonlinear least square method using sub-space trust regions was more accurate then using regularization techniques. However, for test cases within this procedure, regularization methods are comparable, such as the least squares conjugate gradient method with L-curve regularization. This is because the amount of current required can be minimized. If a conventional optimization routine is applied, the current demand can drastically increase due to the ill-posed nature of the inverse problem. To decrease the instability involved in finding a solution, the regularization technique is applied to find more stable solutions. This improves the feasibility of the solution. In addition, it is faster, when applied to linear problems. However, minimal error is still imperative. Therefore, the optimization methods are applied as well for comparison. The following section defines the test case used to illustrate the procedures of this solution process.

3. THE MPAD TEST CASE

The motivating test case for the development of VFG is the research of next generation aircraft concepts that utilize the interaction of magnetostatic fields and charged particle flows for heat and drag reduction. The Lorentz force of an appropriately generated field can steer the flow of charged air particles away from the surface of the aircraft. The Boeing Company and other interested research and development institutions have considered that this MPAD concept could provide magnetic thermal protection to replace or simplify the complex heat protection materials envisioned for a next generation Shuttle replacement or a high altitude, hypersonic aircraft or other applications. The goal is to reduce heat transfer on a flat plate in a high-speed airflow environment. This plate represents the aircraft outer skin panels of an inlet ramp or nose section. Specific to a design problem, the panel is 1.22 meters by 1.22 meters. The problem consists of two separate test cases. The first is to produce a uniform magnetic field of 0.5 Tesla normal to the surface of the panel at a distance of 50.8 millimeters from the surface; this is the Normal Field case. The second case is identical to the first with the exception that the uniform field's orientation should be parallel to the surface, the Parallel Field case. The field error for each case must not exceed 10%. A study was previously conducted to investigate the feasibility of several conventional designs for solving this problem. These designs included a parallel wire conductor array, Halbach array, and other conceptual designs. The designs from this study were able to produce parallel field orientation, however, not without some major disadvantages. Consequently, the identification of the magnetic systems required must be completed to feasibly implement this new magneto-plasma-aerodynamic technology. An added challenge is to devise a single system capable of producing this field pattern oriented parallel to the panel and normal to the panel without altering the physical structure. Operating this system would be advantageous to requiring two systems, one for each field pattern orientation. Furthermore, this ability to dynamically change the field pattern during operation could be used to control the aerodynamic forces of lift and drag applied to the aircraft in order to provide magnetic field flight control for very revolutionary research and development endeavors. The VFG algorithm is specifically suited to conceive such a system and was employed. The following is an outline of the process the algorithm uses to solve the MPAD test case that consists of two cases, the Normal and Parallel Field.

Both the Normal and Parallel Field cases provide the desired field vectors at specific locations relative to the unknown magnetic system. By utilizing the area allocated for the magnetic system as specified, the respective *VFG source radius* can be determined for a specific set of *VFG matrix dimensions*. Particular to the square

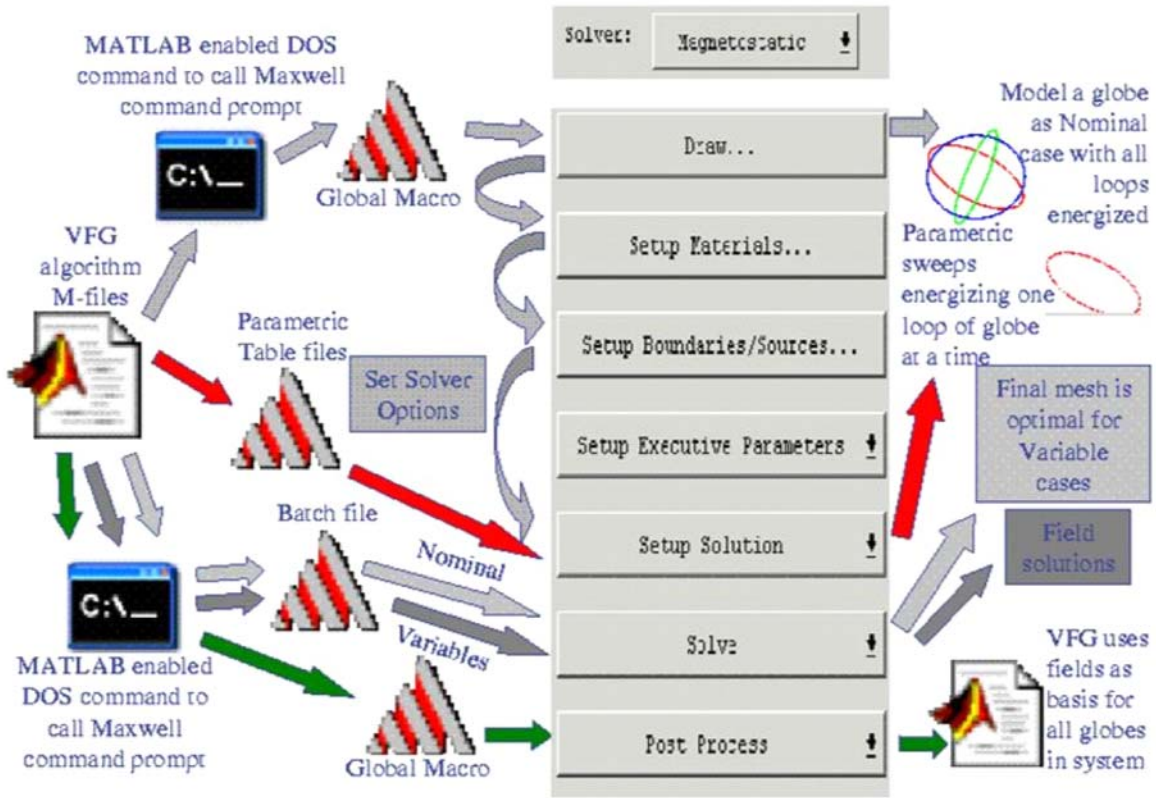

Figure 4: Diagram of process used to integrate Maxwell 3D into VFG algorithm.

geometry of this test case, the matrix would have to be of dimension $m \times m \times n$ in a Cartesian space. Therefore, only two values would have to be permutated, *m* and *n*, and the resulting *VFG source radius*, in meters, can be computed based on the number of sources, forcing the overall size of the magnet structure to remain within the boundaries of a 1.22 by 1.22 meter surface area. Technically, the domain bounds of the matrix dimensions *m* and *n* are optional. However, it is practical that there would be physical limitations on the size of the VFG sources. Specifically, a minimum radius of 0.060 meters was selected. This equates to approximately a maximum limit of 10 on *m*. Arbitrarily, *n* was restricted from 1 to 2. This was reasonable since the application would benefit from the minimum depth of the magnetic source for installation. Therefore, for the first design phase, the set of *VFG matrix dimensions* to be iteratively swept through would be a permutations of $\mathbf{m} = \{1, 2, \ldots, 10\}$ and $\mathbf{n} = \{1, 2\}$, thus limiting the *VFG source radius* to range from 0.6096 to 0.061 meters. Because the first phase is focused only on the number of sources, the conductor model type used will be the infinitely thin conductor loop model. This model utilizes the analytical equations for a one-dimensional current loop and is much faster than employing the Maxwell 3D integration process.

Once the VFG algorithm is executed to derive the given set of design solutions, the results are examined to determine which options provided the best solution. This examination identified the optimal solution to be a matrix of 10 by 10 by 2 “globes” or sources, which equates to a loop radius of 0.061 meters. This result will be used to narrow the searched solution space for the next phase of the design procedure, which will be conducted to vary other design variables. The selection process that derived this optimal configuration is automated within the algorithm, requiring only a set of specified criteria and tolerances. These criteria are the field error of measurements that have a non-zero desired specification and the field error of measurements that are specified to be zero. Additionally a secondary criterion for designs that satisfy the error criteria is that the total current demand be minimized. Therefore, after solving both the Normal and Parallel Field cases selected for this MPAD test case, the percent error of the desired flux density components are measured and compared, depending on the number of sources and the solver utilized. This can be found in Figure 5(a). Those systems that satisfy the criteria of less than 10% maximum non-zero flux density error and a maximum error of less than 0.025 Tesla (%5 of maximum specified field) for specified zero flux densities lie within the acceptance region. It is important to note that this unusual mapping of the error is useful for quick visual inspection of where the designs lie relative to one another and the desired performance level. The ultimate goal of using such a plot is to identify acceptable designs based on the zero and non-zero specified field error, simultaneously. These acceptable designs are then compared to determine the optimal system based on the total demand in current and the flexibility of the system to satisfy all test cases, as seen in Figure 5(b). This means that no matter what the performance level, a design must be acceptable for both test cases, Normal and Parallel.

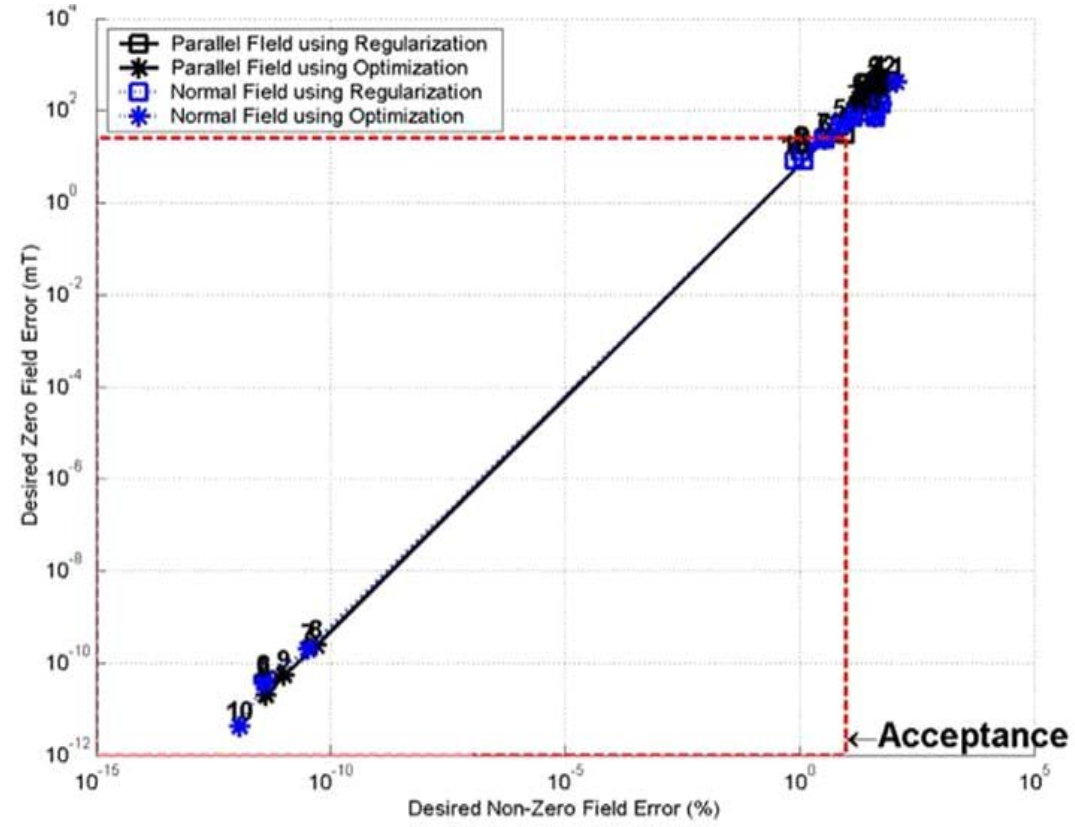

(a)

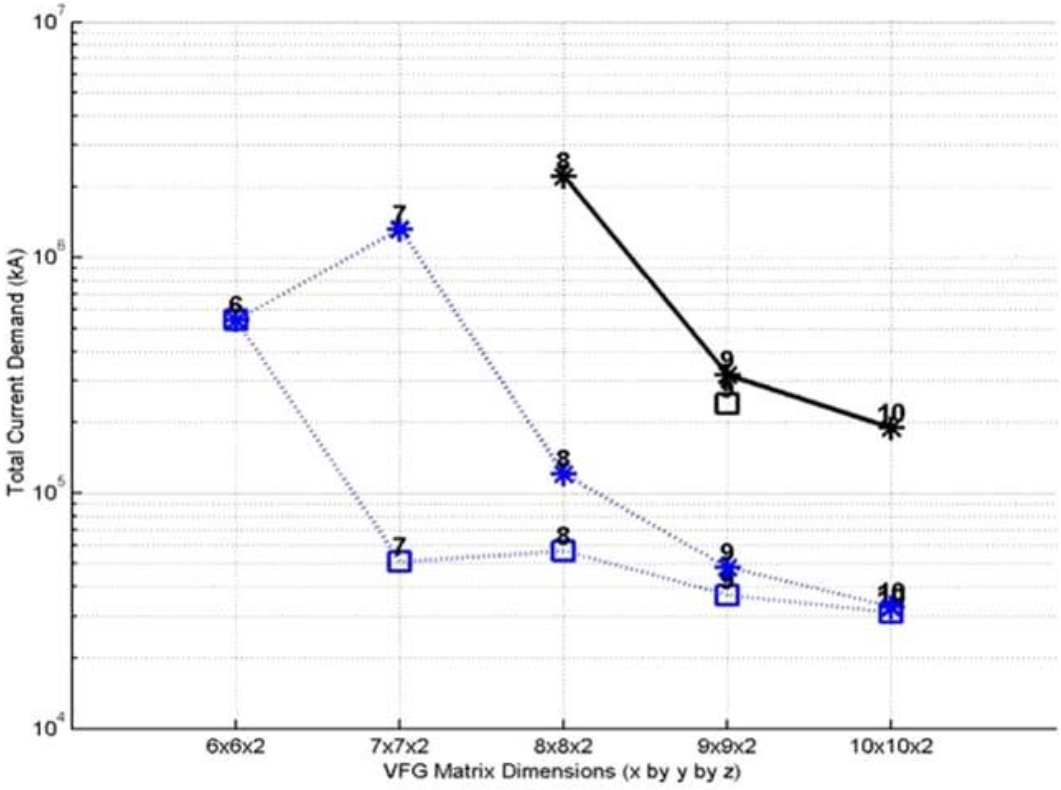

(b)

Figure 5: Finding optimal VFG solution. (a) Field error results for VFG solutions. Those satisfying desired criteria lie within acceptance region. (b) Current demands of acceptable solutions from Figure 5(a) are used to determine optimal solution.

Now that the matrix dimensions have been determined, the next design phase is to determine the *conductor radius* and *VFG loop order*. The nonlinear solver was applied to the design case selected from the first design phase. Fortunately, there are only six possible permutations of the loop order. Therefore the algorithm is executed again six times for each case using a different *VFG loop order* and solving for the conductor radius and excitation current using a nonlinear solver. For the MPAD design problem, a combination solver is applied. This combination solver utilizes an outer optimization of the *conductor radius* using nonlinear least squares method that relies on linear least squares with L-curve regularization of the loop currents as the inner function evaluation. This method is faster than attempting to solve for both the *conductor radius* and loop currents simultaneously. Using the same process of minimizing field errors and limiting current demand, the optimal conductor radius is 9.993 millimeters and the *VFG loop order* is 132 - meaning that the outermost loop of the source lies in the *yz* plane; the middle, in the *xy*; and the innermost, in the *xz*. Although all of the required design variables have been determined, it does not supply a sufficient design solution. Due to the error associated with the infinitely thin wire model of the source that is being utilized for the sake of speed, the solution of excitation currents cannot be trusted. This is demonstrated as part of the algorithm since Maxwell 3D is automated to provide verification of field production after the second phase field synthesis. The design parameters of the infinitely thin wire model are utilized to construct an equivalent 3D model in Maxwell. The conductors now have a cross sectional area and the radius of that area is specified by the *conductor radius*. This test is executed for conductor materials of copper and a perfect conductor. The field errors of the Maxwell models versus those of the field specifications of the Parallel Field case are given in Figure 6 for the copper conductor. The Normal Field case is not displayed because the results are practically identical. Consistent with the Normal Field case, the perfect conductor has a larger variation then the copper conductor does. The amount of error associated with this comparison substantiates that integrating Maxwell 3D into the algorithm to evaluate the field distribution is essential to correct for the field error between the different model solutions. This will remove the discrepancy seen in Figure 6. However, the purpose of this design phase was to determine the *conductor radius* and *VFG loop order*. From previous experimentation, it has been shown that the fields of the analytical and finite element models are of the same magnitude when using the same conductor radius, [1].

Now that all of the design variables have been determined, the third and final phase of this process is to apply a linear solver to determine the final excitation currents using the Maxwell 3D model on each case and for each *conductor model type*, copper and perfect conductor. Using the automation scheme introduced earlier, the analytical mathematical model and its evaluation are replaced by the finite element analysis. The resulting field errors for both test cases are negligible, less than 10^{-12} Tesla. The result is the design of Figure 7 which, when excited according to the VFG solutions, can produce either the Normal or Parallel field patterns specified for magneto-plasma-aerodynamics.

4. CONCLUSIONS

Variable Field Generation uses field synthesis methods to inversely determine the excitation of specific magnetic sources for production of desired magnetic field patterns. To accomplish this objective, VFG adapts a current loop source-searching algorithm devised for non-evasive reconstruction of current distributions and adopts a magnetic source model similar to magnetic noise cancellation devices for helicopter compasses. The integration of such disparate concepts provides a unique solution to this specific application in that it also offers the ability to dynamically alter the magnetic field pattern produced by a designed system. However, this algorithm is not the only solution to the synthesis of magnetic designs. There are many other inverse problem solution methods, but VFG was developed with the distinctive purpose of facilitating the use of MPAD for flight control, which requires variable field patterns. As enabling technologies, such as superconductor performance and magnet infrastructure, advance, field synthesis tools such as this will do well to inspire new and unique magnetic designs and applications.

REFERENCES

1. N.R. Brooks, *Magnetostatic Field Synthesis for Magneto-Plasma-Aerodynamic Devices*, Ph.D. Dissertation, Florida A&M University, 2004.

2. N. Brooks and T. Baldwin, Methodology for universal synthesis of magnetic designs based on field specifications, *Proceedings of the 34th Southeastern Symposium on System Theory*, pp. 113 –117, March 2002.

3. W.R. Smythe, *Static and Dynamic Electricity.* McGraw-Hill, New York, 1950.

4. N.R. Brooks and T.L. Baldwin, Universal magnetic inversion scheme to design novel superconducting magnet systems. *IEEE Trans. Appl. Superconductivity* (2003) **13**, 1676 –1679.

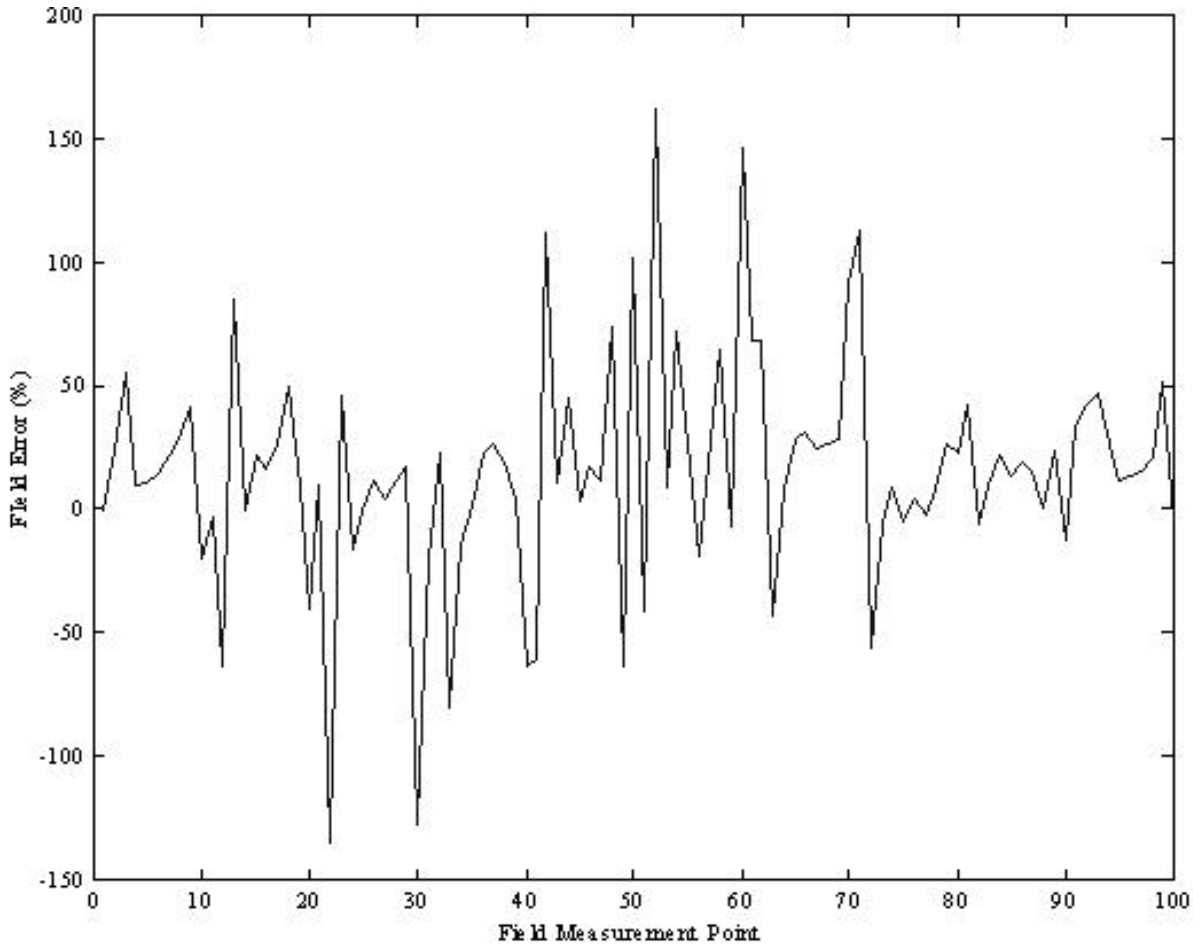

Figure 6: Field error of Parallel Field case using thin wire model results for finite radius copper model.

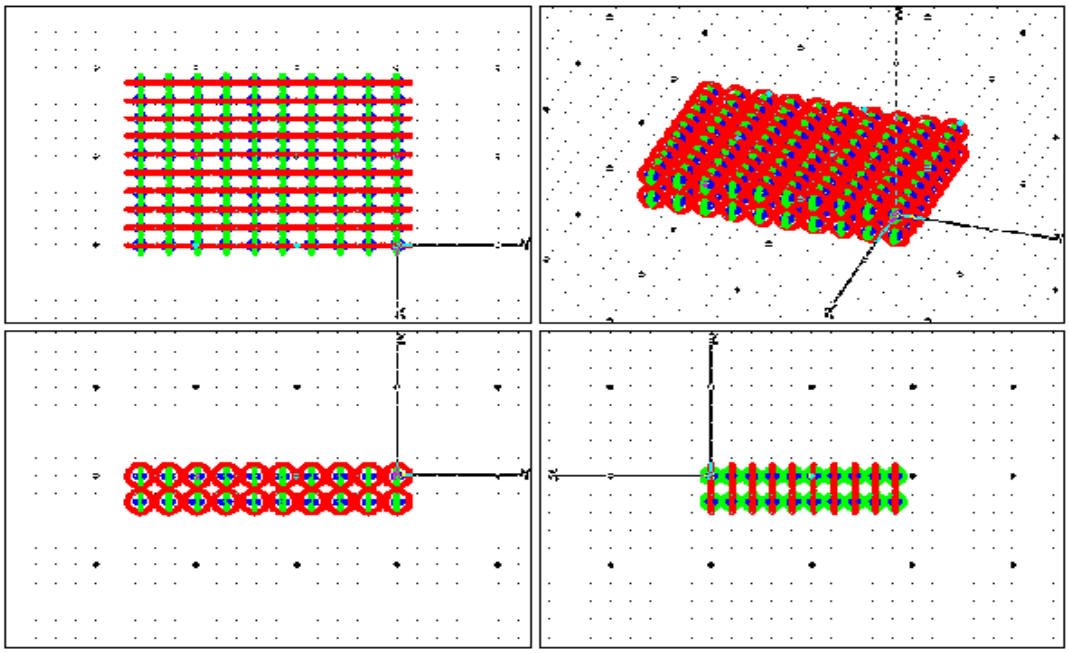

Figure 7: Illustration of 10 by 10 by 2 VFG matrix in Maxwell 3D using finite radius conductor models. This configuration was determined as the optimal design to enable production of both the Normal Field and Parallel Field requirements of the MPAD test case.